Coupling of electrostatic ion cyclotron and ion acoustic waves in the solar wind

T. Sreeraj,[1,a)] S. V. Singh,[1,2,b)] and G. S. Lakhina[1,2,c)]
[1]*Indian Institute of Geomagnetism, Navi Mumbai, India*
[2]*University of the Western Cape, Bellville 7535, Capetown, South Africa*

(Received 23 May 2016; accepted 23 July 2016; published online 12 August 2016)

The coupling of electrostatic ion cyclotron and ion acoustic waves is examined in three component magnetized plasma consisting of electrons, protons, and alpha particles. In the theoretical model relevant to solar wind plasma, electrons are assumed to be superthermal with kappa distribution and protons as well as alpha particles follow the fluid dynamical equations. A general linear dispersion relation is derived for such a plasma system which is analyzed both analytically and numerically. For parallel propagation, electrostatic ion cyclotron (proton and helium cyclotron) and ion acoustic (slow and fast) modes are decoupled. For oblique propagation, coupling between the cyclotron and acoustic modes occurs. Furthermore, when the angle of propagation is increased, the separation between acoustic and cyclotron modes increases which is an indication of weaker coupling at large angle of propagation. For perpendicular propagation, only cyclotron modes are observed. The effect of various parameters such as number density and temperature of alpha particles and superthermality on dispersion characteristics is examined in details. The coupling between various modes occurs for small values of wavenumber. *Published by AIP Publishing.*
[http://dx.doi.org/10.1063/1.4960657]

I. INTRODUCTION

The electrostatic ion cyclotron (EIC) waves are the low-frequency (frequency near ion gyrofrequency) waves which propagate nearly perpendicular to the ambient magnetic field and have a small wavenumber along the magnetic field. In a multi-ion plasma, EIC waves can have frequencies near their respective ion gyrofrequencies. These waves were first observed by D'Angelo and Motley,[1] Motley and D'Angelo[2] in laboratory plasmas and subsequently have been observed in high latitude ionosphere by Mosier and Gurnett.[3] EIC waves have been investigated in a variety of laboratory plasma conditions.[4–7] Based on the observations that disruption of electron flux occurred in concordance with EIC wave frequency, it was concluded that large amplitude EIC waves can trap electrons.[5]

In the auroral region, EIC waves have been observed frequently by various satellites, e.g., S3–3,[8–10] ISEE-1,[11] Viking,[12] Polar,[13] and FAST.[14] First observations of large amplitude EIC waves near the Earth's dayside magnetopause were presented by Tang *et al.*[15] by using the data from Time History of Events and Macroscale Interactions during Substorms (THEMIS) satellites. These EIC waves were observed in a boundary layer in the magnetosphere adjacent to the magnetopause where reconnection occurred. Further, plasma density gradient was identified as a possible source of free energy for these EIC waves. EIC waves have also been observed at low altitudes in diffuse aurora[16] and topside ionosphere.[17] The possible free sources of energy to generate EIC waves are field aligned currents; ion beams; velocity shear; and relative streaming between ions, electron drifts, and density gradients.[9,11,15,18–26] Kindell and Kennel[18] showed that the field aligned currents can drive the EIC waves in the auroral arc. Using the high resolution FAST satellite data, Cattell *et al.*[14] showed that electron drift, i.e., field aligned current can act as a source of EIC waves in the auroral zone. Satellite measurements also showed observations of EIC waves even though the field aligned currents were below the critical threshold for their generation. Later on, it was shown[27] that if perpendicular velocity shear in the ion flow along the magnetic field lines was taken into account, then EIC waves could grow even in the absence of field aligned currents. The study of EIC waves is important from the point of view that they can provide perpendicular heating of the ions in the Earth's magnetosphere and are of importance in understanding and maintaining the boundary layers.[15] Tsurutani and Thorne[28] suggested that the He^{++} in the magnetosheath may be transported inward by resonating with the EIC waves as they are capable of inducing the required rapid inward diffusion of typical magnetosheath ions. Further, H^{+} ions may also be heated and diffused by EIC waves.

EIC waves in multi-component plasmas have also attracted great deal of interest from theoretical plasma physicists and have been studied in a variety of plasmas. Using kinetic theory, Chow and Rosenberg[29] showed that for the excitation of both the positive and negative ion modes, the critical electron drift velocity decreased with increase in the relative density of the negative ions. On the other hand, the frequencies and growth rates of both the unstable modes increase with the relative density of negative ions. EIC wave excitation in a plasma containing negatively charged dust particles has been investigated both experimentally and theoretically by Barkan *et al.*,[4] and Chow and Rosenberg.[30] Sharma

[a)]Electronic mail: sreerajt13@iigs.iigm.res.in
[b)]Electronic mail: satyavir@iigs.iigm.res.in
[c)]Electronic mail: gslakhina@gmail.com

and Sharma[31] studied the excitation of EIC waves by an ion beam in a two-component, collisionless plasma which was extended by Sharma *et al.*[32] to include collisions. Sharma *et al.*[33] developed a theoretical model to study the excitation of higher harmonics of ion-cyclotron waves in a plasma cylinder with heavy negative ions. The propagation characteristics of electrostatic ion cyclotron waves have been studied in a homogeneous pair-ion plasma in a cylindrical system.[34] Using the kinetic theory, the observed waves are identified to be ion cyclotron harmonic waves in the intermediate frequency range, whereas in the low-frequency range, a coupled wave of ion cyclotron mode and ion thermal mode is identified. Using a fluid theory, Merlino[35] showed that electrostatic ion cyclotron waves propagating at large angles to the ambient magnetic field can be excited in a magnetized plasma by perpendicular shear in the magnetic field aligned plasma flow. In a uniform plasma, the resonant excitation of EIC modes by the electron drift relative to the ions has been studied by Drummond and Rosenbluth.[36] Lakhina,[23] Gavrishchaka *et al.*,[37,38] and Ganguli *et al.*[27] investigated the effect of parallel velocity shear on the excitation of current-driven ion acoustic and EIC modes. In some of the cases, it was found that the presence of shear can drastically reduce the necessary critical drift velocities for the excitation of these modes. It was also shown that even in the absence of relative electron drift, perpendicular shear in the parallel ion flow could lead to the excitation of multiple ion-cyclotron harmonics.

The low-frequency ion acoustic waves (IAWs) have been observed in the solar wind and various regions of the Earth's magnetosphere.[39–42] These waves have been extensively studied theoretically.[43–45] Mostly, the electrostatic ion cyclotron and ion acoustic waves (IAWs) have been studied independently rather than the focus on coupling of these waves in magnetized plasmas. The study on the coupling between the electrostatic ion cyclotron and ion acoustic waves was carried out in laboratory plasma by Ohnuma *et al.*,[46] where they observed the coupling between EIC and ion acoustic waves near the second harmonic frequency in a quiescent plasma (QP) machine. The recent observations from THEMIS[15] also indicated the possible occurrence of a coupling between EIC and ion acoustic waves.

Solar wind is a stream of charged particles ejected from the Sun and consists of protons, electrons along with an admixture of alpha particles and much less abundant heavier ions. As it turns out, there are two different classes of solar wind—namely, fast solar wind and slow solar wind. The properties and composition of both these types of solar wind vary considerably. In fast solar wind ($V_{sw} \sim 650$ km/s), ions tend to be hotter than both protons and electrons, the protons are hotter than the electrons as well, and the α particles move faster than the protons. Also, in fast solar wind, the proton temperature is anisotropic with $\frac{T_{p\perp}}{T_{p\parallel}} > 1$. On the other hand, for the slow solar wind ($V_{sw} \sim 350$ km/s), electrons are much hotter than ions and the proton temperature anisotropy is opposite to that of fast solar wind.[47–49]

In the solar wind, two different kinds of charged particles, a low energy thermal core and a suprathermal halo which are isotropically distributed at all pitch angles, are found.[50,51] In the fast solar wind, the halo distribution can carry a highly energetic and antisunward moving magnetic field aligned strahl population.[48,52] Both electrons and ion species such as H^+, He^{++}, and other heavier ions present in the solar wind can have suprathermal particle distributions.[53,54] These suprathermal particle distributions can be modelled by kappa distribution. In order to fit the experimentally observed data from OGO-1 and OGO-3 satellites in the magnetosphere, it was Vasyliunas[55] who first postulated this kind of distribution function for the electrons. Thereafter, kappa distribution function has been observed and used in various regions of the magnetosphere and beyond, such as solar wind,[56] magnetosheath,[57] ring current,[58] plasma sheet,[59] magnetosphere of other planets, e.g., Saturn,[60] and also on planetary nebulae.[61] Theoretically, linear ion-acoustic and ion-cyclotron waves in magnetized electron-proton plasma have been studied with electrons having kappa distribution.[43–45] The current driven electrostatic ion-cyclotron instability has been studied in electron-proton plasma with kappa-Maxwellian distributions for electrons and ions.[62] In these articles, coupling between the electrostatic ion cyclotron and ion acoustic waves has not been discussed. In this paper, electrostatic low-frequency waves are studied in a three-component, magnetized plasma composed of electrons, protons, and alpha particles. The electrons are assumed to have superthermal distribution characterised by kappa distribution. Protons and alpha particles are assumed to follow fluid dynamical equations. Our focus will be on the coupling process of ion acoustic and ion cyclotron waves. The parameters from slow solar wind are used for the numerical computation of the dispersion relation characteristics.

The paper is organized as follows: In Section II, a theoretical model to study the low-frequency electrostatic waves in magnetized plasma is presented and dispersion relation is analyzed for special cases of short and long wavelength limits for two-component (electron-proton) magnetized plasma, and a general dispersion relation for three-component plasma is analyzed for parallel and perpendicular propagation. In Section III, numerical results are presented, and conclusion and discussion are given in Section IV.

II. THEORETICAL MODEL

The solar wind plasma is modeled by a homogeneous, collisionless, and magnetized three component plasma comprising of fluid protons (n_p, T_p), fluid heavier ions (n_i, T_i), and suprathermal electrons (n_e, T_e) having κ distribution. Here, n_s and T_s are the number density and temperature of the species s, respectively, where $s = p$, i, and e stand for protons, heavier ions, and suprathermal electrons, respectively. The heavier ions are considered to be doubly charged helium (He^{++}, $z_i = 2$) ions, i.e., alpha particles. The ambient magnetic field is considered to be in the z-direction, i.e., $\mathbf{B}_0 \parallel \mathbf{z}$. For simplicity, we take the propagation vector, $\mathbf{k}$, to be in $x - z$ plane making an angle α to the B_0 (see Figure 1).

For the linear, electrostatic waves propagating obliquely to the ambient magnetic field, the dynamics of both protons and the heavy ions is described by the multi-fluid equations

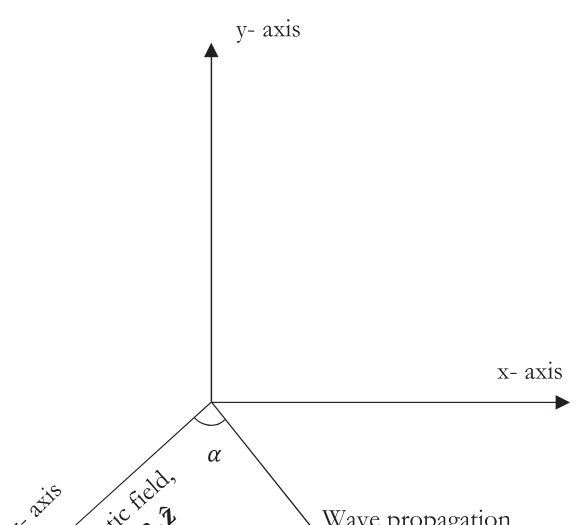

FIG. 1. Geometry.

of continuity, momentum, and the Poisson equation. Thus, the set of governing equations is given by

$$\frac{\partial n_s}{\partial t} + \nabla.(n_s \mathbf{v}_s) = 0, \tag{1}$$

$$m_s n_s \left[\frac{\partial \mathbf{v}_s}{\partial t} + (\mathbf{v}_s.\nabla)\mathbf{v}_s\right] = q_s n_s \left(-\nabla\phi + \frac{\mathbf{v}_s \times \mathbf{B}_0}{c}\right) - \nabla P_s, \tag{2}$$

$$\nabla^2\phi = -4\pi e(n_p + n_i z_i - n_e), \tag{3}$$

where m_s, $\mathbf{v}_s$, P_s, and q_s represent mass, velocity, pressure, and charge of the species $s = p, i$, respectively. The pressure term in our case amounts to $\nabla P_s = \gamma k_B T_s \nabla n_s$, where γ is the ratio of specific heats and k_B is the Boltzmann constant.

The suprathermal electrons are assumed to have κ distribution which is given by[63]

$$f_\kappa(v) = \frac{n_{e0}}{\pi^{\frac{3}{2}}}\frac{1}{\theta^3}\frac{\Gamma(\kappa+1)}{\kappa^{\frac{3}{2}}\Gamma\left(\kappa-\frac{1}{2}\right)}\left(1+\frac{v^2}{\kappa\theta^2}\right)^{-(\kappa+1)}, \tag{4}$$

where κ is the superthermality index, $\Gamma(\kappa)$ is the gamma function with the argument κ, θ is the effective thermal speed of electron given by the expression $\theta = \left[(2\kappa-3)/\kappa\right]^{\frac{1}{2}}(k_B T_e/m_e)^{\frac{1}{2}}$, and n_{e0} is the equilibrium density of energetic electrons. From this definition, it is clear that in order to have meaningful value for the thermal speed, we need to have $\kappa > \frac{3}{2}$.

Zeroth moment of this distribution in the presence of wave potential ϕ gives the perturbed number density of electron, which is

$$n_{e1} = n_{e0}\left[1 - \frac{e\phi}{k_B T_e\left(\kappa-\frac{3}{2}\right)}\right]^{\frac{1}{2}-\kappa}, \tag{5}$$

where the subscripts 0 and 1 stand for unperturbed and perturbed states, respectively. Linearization and simplification of Eqs. (1)–(3) and (5) yield the following general dispersion relation for the low frequency, coupled electrostatic cyclotron (proton and helium), and acoustic (fast and slow) modes:

$$1 + \frac{\omega_{pe}^2}{k^2 v_{the}^2}\frac{2\kappa-1}{2\kappa-3} - \frac{\omega_{pp}^2\left(\omega^2 - \Omega_p^2\cos^2\alpha\right)}{\omega^4 - \omega^2\Omega_p^2 - \gamma k^2 v_{thp}^2\left(\omega^2 - \Omega_p^2\cos^2\alpha\right)} - \frac{z_i^2\omega_{pi}^2\left(\omega^2 - z_i^2\Omega_i^2\cos^2\alpha\right)}{\omega^4 - \omega^2 z_i^2\Omega_i^2 - \gamma k^2 v_{thi}^2\left(\omega^2 - z_i^2\Omega_i^2\cos^2\alpha\right)} = 0. \tag{6}$$

Here, $\omega_{ps} = \sqrt{4\pi n_{s0}e^2/m_s}$ is the plasma frequency, $\Omega_s = eB_0/m_s c$ is the cyclotron frequency, and $v_{\mathrm{ths}} = \sqrt{k_B T_s/m_s}$ is the thermal speed of the sth species, respectively. In the dispersion relation (6), the second term is due to the electrons having kappa distribution, third term represents the protons, and the last term is due to the heavier ions.

A. Two component plasma

It is interesting to note that in the absence of the ions, the dispersion relation given below describes the coupling of ion-acoustic and ion cyclotron modes in pure electron-proton plasma

$$1 + \frac{\omega_{pe}^2}{k^2 v_{the}^2}\frac{2\kappa-1}{2\kappa-3} = \frac{\omega_{pp}^2\left(\omega^2 - \Omega_p^2\cos^2\alpha\right)}{\omega^4 - \omega^2\Omega_p^2 - \gamma k^2 v_{thp}^2\left(\omega^2 - \Omega_p^2\cos^2\alpha\right)}. \tag{7}$$

Eq. (7) is a quadratic in ω^2, and the solution of this can be given as

$$\omega_\pm^2 = \frac{1}{2}\left[B \pm \sqrt{B^2 - 4C}\right] \quad \text{where}$$
$$B = \Omega_p^2 + \gamma k^2 v_{thp}^2 + \frac{\omega_{pp}^2 k^2\lambda_{de}^2(2\kappa-3)}{k^2\lambda_{de}^2(2\kappa-3) + (2\kappa-1)} \quad \text{and}$$
$$C = \Omega_p^2\cos^2\alpha\left(\gamma k^2 v_{thp}^2 + \frac{\omega_{pp}^2 k^2\lambda_{de}^2(2\kappa-3)}{k^2\lambda_{de}^2(2\kappa-3) + (2\kappa-1)}\right). \tag{8}$$

Here, $\lambda_{de} = v_{the}/\omega_{pe}$ is the electron Debye length. Eq. (8) is similar to the equation that has been obtained by Hellberg and Mace,[43] Sultana *et al.*,[44] and Kadijani *et al.*[45] for a two component plasma model of cold protons and superthermal electrons described by kappa distribution. Eq. (8) describes the coupling of ion-acoustic and ion-cyclotron waves in two component plasma. Further, we would like to discuss propagation characteristics of the low-frequency waves by analysing the dispersion relation for special cases, e.g., parallel and perpendicular wave propagation and large and short wavelength limits.

1. Parallel propagation

For parallel propagation ($\alpha = 0°$, i.e., $\cos\alpha = 1$), Eq. (8) reduces to

$$\omega_+^2 = \Omega_p^2, \tag{9}$$

$$\omega_-^2 = \gamma k^2 v_{thp}^2 + \frac{\omega_{pp}^2 k^2 \lambda_{de}^2 (2\kappa - 3)}{k^2 \lambda_{de}^2 (2\kappa - 3) + (2\kappa - 1)}, \tag{10}$$

where the decoupling of ion cyclotron and ion-acoustic modes occurs. Eq. (9) refers to nonpropagating ion-cyclotron mode which is the fluctuation at the proton cyclotron frequency and Eq. (10) refers to ion-acoustic mode.

2. Perpendicular propagation

For perpendicular propagation ($\alpha = 90°$, i.e., $\cos\alpha = 0$), the only surviving root will be

$$\omega_+^2 = \Omega_p^2 + \gamma k^2 v_{thp}^2 + \frac{\omega_{pp}^2 k^2 \lambda_{de}^2 (2\kappa - 3)}{k^2 \lambda_{de}^2 (2\kappa - 3) + (2\kappa - 1)}. \tag{11}$$

Equation (11) corresponds to the ion cyclotron wave with the thermal corrections. The acoustic mode completely disappears. Next, we analyse the dispersion relation given by Eq. (7) in the large and short wavelength limits.

3. Large wavelength limit

In the large wavelength limit, i.e.,

$$\Omega_p^2 \gg \gamma k^2 v_{thp}^2 + \frac{\omega_{pp}^2 k^2 \lambda_{de}^2 (2\kappa - 3)}{k^2 \lambda_{de}^2 (2\kappa - 3) + (2\kappa - 1)},$$

the two roots of Eq. (7) can be written as

$$\omega_+ = \Omega_p + \frac{\sin^2\alpha}{2\Omega_p}\left[\gamma k^2 v_{thp}^2 + \frac{\omega_{pp}^2 k^2 \lambda_{de}^2 (2\kappa - 3)}{k^2 \lambda_{de}^2 (2\kappa - 3) + (2\kappa - 1)}\right], \tag{12}$$

$$\omega_- = \cos\alpha \sqrt{\gamma k^2 v_{thp}^2 + \frac{\omega_{pp}^2 k^2 \lambda_{de}^2 (2\kappa - 3)}{k^2 \lambda_{de}^2 (2\kappa - 3) + (2\kappa - 1)}}. \tag{13}$$

Eq. (12) refers to proton cyclotron mode, and Eq. (13) describes the obliquely propagating ion acoustic mode in a magnetized electron-ion plasma. These results are identical to Hellberg and Mace,[43] Sultana *et al.*,[44] and Kadijani *et al.*[45]

4. Short wavelength limit

In the short wavelength limit, i.e.,

$$\Omega_p^2 \ll \gamma k^2 v_{thp}^2 + \frac{\omega_{pp}^2 k^2 \lambda_{de}^2 (2\kappa - 3)}{k^2 \lambda_{de}^2 (2\kappa - 3) + (2\kappa - 1)},$$

the two roots of Eq. (7) can be written as

$$\omega_+ = \sqrt{\gamma k^2 v_{thp}^2 + \frac{\omega_{pp}^2 k^2 \lambda_{de}^2 (2\kappa - 3)}{k^2 \lambda_{de}^2 (2\kappa - 3) + (2\kappa - 1)}}, \tag{14}$$

$$\omega_- = \Omega_p \cos\alpha. \tag{15}$$

In the short wavelength limit, the mode given by Eq. (14) behaves like ion-acoustic mode in unmagnetized plasma and the other mode described by Eq. (15) is the oblique ion cyclotron fluctuation.

We now numerically investigate the dispersion relation for two-component plasma given by Eq. (7). For this purpose, we have normalised the frequencies by cyclotron frequency of proton, Ω_p, wavenumber by Larmor radius of proton, ρ_p, given by the expression $\rho_p = v_{thp}/\Omega_p$. The parameters chosen are $\frac{T_e}{T_p} = 5$, $\gamma = 3$, and $\kappa = 2$. Ratio of plasma frequency to cyclotron frequency of proton is taken to be 5000.[64,65] The results of the findings are presented in Figure 2. As mentioned in the text earlier, for parallel wave propagation, i.e., $\alpha = 0°$, the two different modes, viz., ion cyclotron (solid curve parallel to the x-axis, branch 1) and ion acoustic (solid straight line passing through origin, branch 2) modes decouple. These two modes are represented by Eqs. (9) and (10), respectively. The effect of obliqueness is also examined on the dispersion characteristics of ion-cyclotron and ion-acoustic waves in two component plasma. First, we have analysed Eq. (7) for the case of $\alpha = 15°$, for which the dispersion relation curve gets modified as shown by short dashed curves in Fig. 2. It is seen that the coupling between the ion cyclotron and ion acoustic modes occurs as the wave propagates at an angle to the ambient magnetic field. The short-dashed curve starting at $\omega/\Omega_p = 1.0$ is the ion cyclotron mode which is modified by acoustic mode (given by Eq. (12)). The obliquely propagating ion-acoustic mode (given by Eq. (13)) is represented by short-dashed curve starting from $\omega/\Omega_p = 0.0$. Further increase in the angle of propagation (as shown by long dashed curves in Fig. 2 with $\alpha = 30°$) weakens the coupling as the gap between the two modes widens and continues to weaken for $\alpha = 45°$ and $\alpha = 60°$ (not shown here). The coupling completely vanishes at $\alpha = 90°$ (dashed dotted curve)

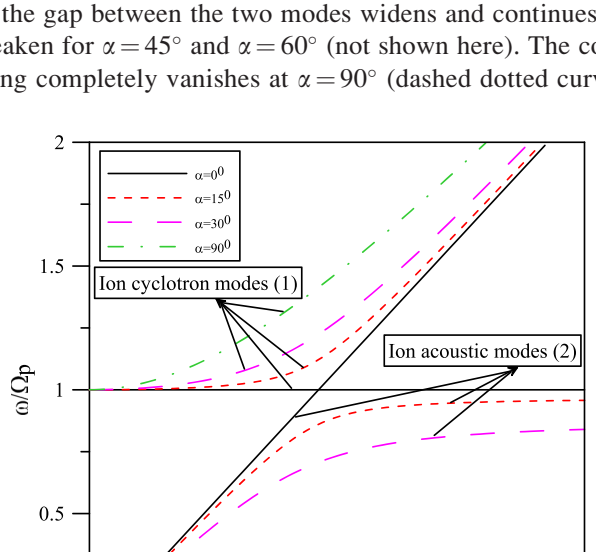

FIG. 2. Dispersion characteristics of the electrostatic ion cyclotron and ion acoustic modes in electron-ion plasma for various angles of propagation. Other parameters are $T_e/T_p = 5$, $\gamma = 3$, and $\kappa = 2$.

as only ion-cyclotron wave remains and ion-acoustic mode disappears which is in agreement with Eq. (11).

B. Three component plasma

The analysis carried out above for two-component plasma will help us in identifying the various modes of plasma given by the general dispersion relation (6) in a three-component plasma which cannot be solved analytically. However, we would like to discuss further the special cases where analytical expressions are tractable and various modes can be identified.

1. Parallel wave propagation

For the case of parallel propagation ($\alpha = 0°$, i.e., cos $\alpha = 1$) of the various modes, the general dispersion relation (6) reduces to the following:

$$\left(\omega^2 - \Omega_p^2\right)\left(\omega^2 - z_i^2\Omega_i^2\right)\left[1 - \frac{\omega_{pp}^2}{\left(1 + \frac{\omega_{pe}^2}{k^2 v_{the}^2}\frac{2\kappa - 1}{2\kappa - 3}\right)\left(\omega^2 - \gamma k^2 v_{thp}^2\right)} - \frac{z_i^2\omega_{pi}^2}{\left(1 + \frac{\omega_{pe}^2}{k^2 v_{the}^2}\frac{2\kappa - 1}{2\kappa - 3}\right)\left(\omega^2 - \gamma k^2 v_{thi}^2\right)}\right] = 0. \tag{16}$$

It is obvious from the above Eq. (16) that the proton-($\omega = \pm\Omega_p$) and helium-($\omega = \pm\Omega_i$) cyclotron modes (as shown by the first and second terms, respectively) decouple from the acoustic modes given by third term in the square bracket. It has to be pointed out that for parallel propagation of the electrostatic waves the two cyclotron modes are non-propagating, i.e., they represent fluctuations at the proton and helium cyclotron frequency, respectively. Therefore, the third term inside the square brackets of Eq. (16) is further analyzed which is quadratic equation in ω^2 and can be solved analytically. The two roots of the equations are given by the expressions

$$\omega_{\pm}^2 = \frac{1}{2}\left[B_1 \pm \sqrt{B_1^2 - 4C_1}\right], \quad \text{where}$$

$$B_1 = \gamma k^2 v_{thp}^2 + \gamma k^2 v_{thi}^2 + \frac{\left(\omega_{pp}^2 + z_i^2\omega_{pi}^2\right)k^2\lambda_{de}^2(2\kappa - 3)}{k^2\lambda_{de}^2(2\kappa - 3) + (2\kappa - 1)} \quad \text{and}$$

$$C_1 = \gamma^2 k^4 v_{thp}^2 v_{thi}^2 + \frac{\gamma\left(v_{thi}^2\omega_{pp}^2 + v_{thp}^2 z_i^2\omega_{pi}^2\right)k^4\lambda_{de}^2(2\kappa - 3)}{k^2\lambda_{de}^2(2\kappa - 3) + (2\kappa - 1)}. \tag{17}$$

The $\omega_{\pm}$ refers to the fast and slow acoustic modes, respectively. For parallel propagation, the fast and slow acoustic modes are not affected by the presence of magnetic field. Next, we consider the case of perpendicular propagation of the waves.

2. Perpendicular wave propagation

For wave propagation perpendicular to the ambient magnetic field, i.e., for $\alpha = 90°$, i.e., cos $\alpha = 0$, the general dispersion relation Eq. (6) reduces to the following:

$$1 - \frac{\omega_{pp}^2}{\left(1 + \frac{\omega_{pe}^2}{k^2 v_{the}^2}\frac{2\kappa - 1}{2\kappa - 3}\right)\left(\omega^2 - \Omega_p^2 - \gamma k^2 v_{thp}^2\right)} - \frac{z_i^2\omega_{pi}^2}{\left(1 + \frac{\omega_{pe}^2}{k^2 v_{the}^2}\frac{2\kappa - 1}{2\kappa - 3}\right)\left(\omega^2 - z_i^2\Omega_i^2 - \gamma k^2 v_{thi}^2\right)} = 0. \tag{18}$$

The above equation is quadratic in ω^2 which has four roots. The algebraic manipulation leads to the following roots of Eq. (18):

$$\omega_{\pm}^2 = \frac{1}{2}\left[B_2 \pm \sqrt{B_2^2 - 4C_2}\right], \quad \text{where}$$

$$B_2 = \Omega_p^2 + z_i^2\Omega_i^2 + \gamma k^2 v_{thp}^2 + \gamma k^2 v_{thi}^2 + \frac{\left(\omega_{pp}^2 + z_i^2\omega_{pi}^2\right)k^2\lambda_{de}^2(2\kappa - 3)}{k^2\lambda_{de}^2(2\kappa - 3) + (2\kappa - 1)} \quad \text{and}$$

$$C_2 = \left(\Omega_p^2 + \gamma k^2 v_{thp}^2\right)\left(z_i^2\Omega_i^2 + \gamma k^2 v_{thi}^2\right) + \frac{\left(z_i^2\Omega_i^2 + \gamma k^2 v_{thi}^2\right)\omega_{pp}^2 k^2\lambda_{de}^2(2\kappa - 3)}{k^2\lambda_{de}^2(2\kappa - 3) + (2\kappa - 1)} + \frac{\left(\Omega_p^2 + \gamma k^2 v_{thp}^2\right)z_i^2\omega_{pi}^2 k^2\lambda_{de}^2(2\kappa - 3)}{k^2\lambda_{de}^2(2\kappa - 3) + (2\kappa - 1)}. \tag{19}$$

The $\omega_{\pm}$ in Eq. (19) gives the relation for cyclotron modes for protons and helium ions, respectively, which are modified by the acoustic contribution. In Sec. III, the general dispersion relation (6) will be analyzed numerically.

III. NUMERICAL RESULTS

In this section, the numerical results are presented on the coupling of various modes, and the effect of nonthermality, density, and temperature of ions on the dispersive properties of the modes is also examined. For numerical analysis, we have normalised the general dispersion relation by the following parameters: frequencies by cyclotron frequency of proton, Ω_p, and wavenumber by Larmor radius of proton, ρ_p, given by the expression $\rho_p = \frac{v_{thp}}{\Omega_p}$. For the fast solar wind, $\frac{T_p}{T_e} \geq 1$, $\frac{T_i}{T_p} \geq 1$, and for the slow solar wind, $\frac{T_p}{T_e} \leq 1$, $\frac{T_i}{T_p} \geq 1$.[47] It was shown by Maksimovic *et al.*[66] that κ can take the value from 2 to 6. The recent survey for the value of kappa index undertaken by Livadiotis[67] for various space plasmas has shown that kappa value for solar wind can vary from 1.5 to 7. From

the satellite observations, it can be deduced that the ratio of plasma to cyclotron frequencies of proton is nearly 5000.[64,65] For numerical computations of the dispersion relation (6), we have taken slow solar wind parameters at 1AU which are specified for each figure. For parallel propagation of waves in electron-ion magnetized plasmas, it is relatively easier to analyze a dispersion relation. However, multi-components and oblique propagation of waves in magnetized plasmas make the dispersion relation complex and difficult to analyze analytically. Therefore, it is necessary to do the numerical analysis of the dispersion relation and bring out the characteristics of the various wave modes. We now undertake a parametric investigation of the dispersion relation (6) which will be analysed for effect of obliqueness, ion concentration, superthermality index, and temperature of ions on the characteristics of the various modes. To start with, the dispersion relation Eq. (6) is analysed for parallel propagation, i.e., $\alpha = 0^\circ$, and results are presented in Figure 3(a). The typical chosen parameters corresponding to the slow solar wind are $n_i/n_e = 0.05$, $T_e/T_p = 5$, $T_i/T_p = 2$, $\gamma = 3$, and $\kappa = 2$. It is clearly seen in Figure 3(a) that the four modes, namely, proton-cyclotron (solid curve, branch 1), helium-cyclotron (short dashed curve, branch 2) modes, fast ion-acoustic (dashed-dashed dotted-dotted curve, branch 3), and slow ion-acoustic (long dashed curve, branch 4) decouple at parallel propagation. We have purposely named various wave modes as branches 1–4 for the case of parallel propagation as they will come in handy for oblique propagation cases where coupling of the modes occur. It has to be pointed out here that only physically acceptable solution for parallel propagation are fast and slow acoustic modes. Since we have normalised the frequency with respect to proton cyclotron frequency, parallel lines at $\omega/\Omega_p = 1$ and $\omega/\Omega_p = 0.5$ ($m_{He}/m_p = 4$) represent proton (solid line) and helium cyclotron (dashed line) nonpropagating modes, respectively. The above results are in sync with Eq. (16) as the first two terms on the left hand side describe the proton and helium cyclotron modes, respectively. The fast and slow ion-acoustic modes are the solutions ($\omega_\pm$) of the third term and are given by Eq. (17), respectively.

In Figure 3(b), the effect of obliqueness is examined on the dispersion relation (6). It must be emphasized here that we start with small angle of propagation, $\alpha = 5^\circ$, so that intricate coupling process between the acoustic (fast and slow) and cyclotron (proton and helium) modes can be delineated properly. Here, the plasma parameters are the same as for Figure 3(a). It is obvious from the figure that as the wave propagates oblique to the ambient magnetic field, the coupling between cyclotron and acoustic modes occurs. Further, the proton cyclotron (branch 1) mode couples with two modes, i.e., fast ion-acoustic (branch 3) mode at $k\rho_p \approx 0.45$ and slow ion-acoustic (branch 4) mode at $k\rho_p \approx 0.8$. These two couplings are marked in this and subsequent figures by circles with labels 1 & 3 and 1 & 4, respectively. On the other hand, helium cyclotron mode (branch 2) couples with fast

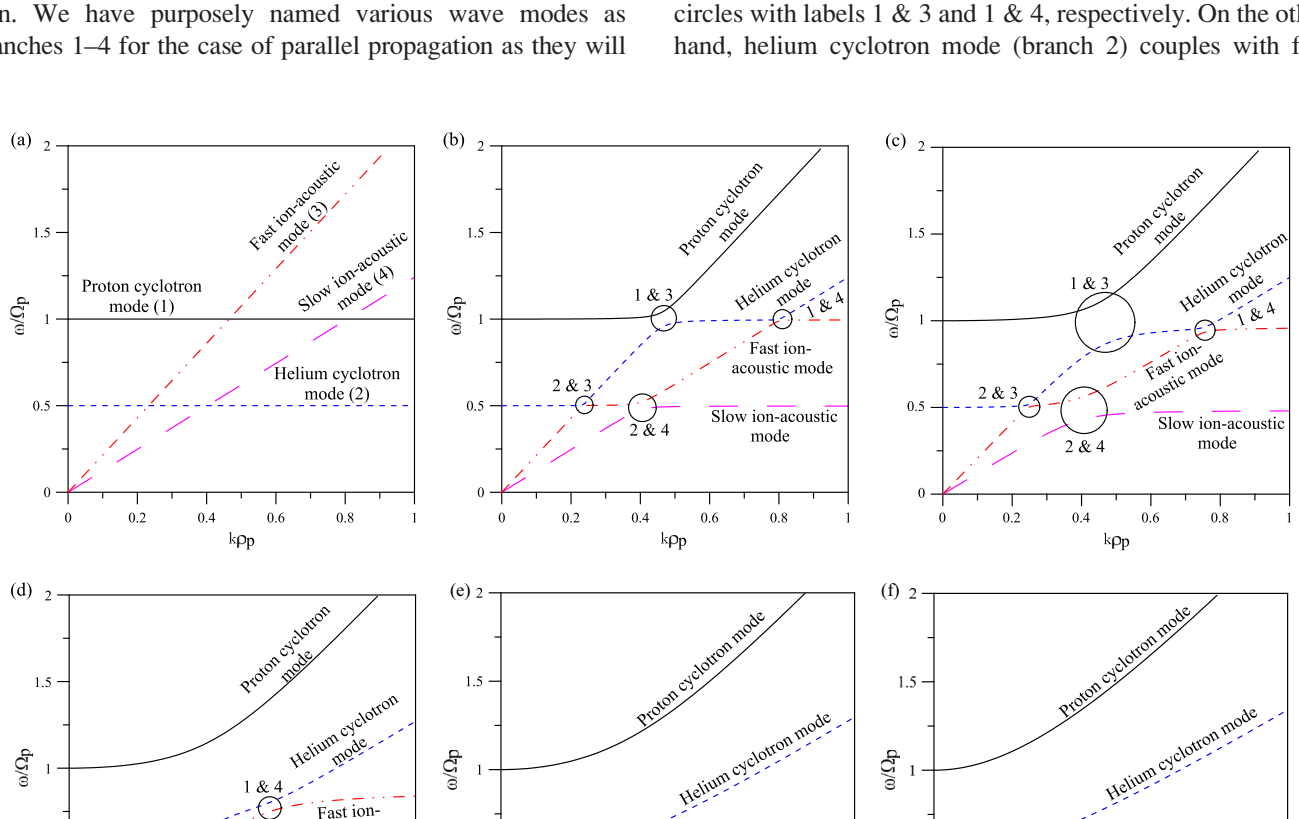

FIG. 3. Dispersion characteristics of the electrostatic ion cyclotron and ion acoustic modes at different angle of propagation, $\alpha = 0^\circ$ (a), 5° (b), 15° (c), 30° (d), 45° (e), and 90° (f) for the slow solar wind parameters $\frac{n_i}{n_e} = 0.05$, $\frac{T_e}{T_p} = 5$, $\frac{T_i}{T_p} = 2$, $\gamma = 3$, and $\kappa = 2$.

ion-acoustic (branch 3) mode at $k\rho_p \approx 0.24$ and with slow ion-acoustic (branch 4) mode at $k\rho_p \approx 0.41$. The couplings are marked in this and subsequent figures by circles with labels 2 & 3 and 2 & 4, respectively. Further, the proton cyclotron mode couples with the two acoustic modes at larger value of $k\rho_p$ as compared to the helium cyclotron mode.

In Figure 3(c), we have shown the results for propagation angle, $\alpha = 15°$, for the same values of parameters as in Figure 3(a). It is observed that coupling between proton-cyclotron (branch 1) and fast ion acoustic (branch 3) modes weakens as gap between the two widens (labelled 1 and 3). Similarly, coupling weakens between helium (branch 2) and slow-ion-acoustic (branch 4) modes (labelled 2 and 4); however, gap is smaller as compared to branches 1 and 3. On the other hand, stronger coupling exists between branches 1 & 4 and 2 & 3. The coupling between branches 1 & 3 and 2 & 4 further weakens at an angle of propagation, $\alpha = 30°$ (Figure 3(d)), but coupling is still strong between branches 2 & 3 and 1 & 4. Increase in angle of propagation, $\alpha = 45°$, further weakens the coupling as can be gauged by the widening gaps (Figure 3(e)). There is no coupling between the various branches at an angle of propagation, $\alpha = 60°$ (not shown here). Finally, at exactly perpendicular propagation ($\alpha = 90°$), both the acoustic (slow and fast) modes disappear and only proton and helium cyclotron modes exist (Figure 3(f)) which can be corroborated with Eq. (19). Here, $\omega_{\pm}$ refers to proton and helium cyclotron modes.

The effect of number density of helium ions is studied in Figure 4 for the parameters of Figure 3(a) and angle of propagation, $\alpha = 30°$. The normalized helium ion density is varied from $n_i/n_e = 0.05$–0.3. It is observed that frequency and phase speed of proton cyclotron, fast and slow ion acoustic modes do not change significantly with the increase in the concentration of helium ions. However, for a fixed value of the wavenumber, the frequency and phase speed of the proton cyclotron and fast ion acoustic modes decreases slightly,

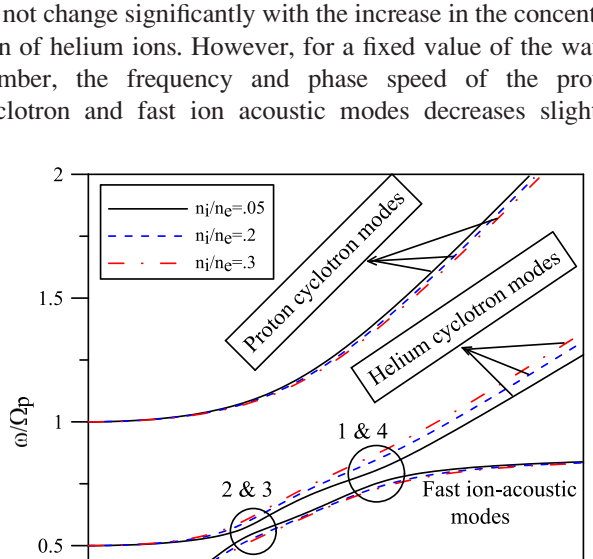

FIG. 4. Dispersion relation curves for variations in number density of Helium ions to protons for propagation angle $\alpha = 30°$. The other parameters are the same as in Figure 3.

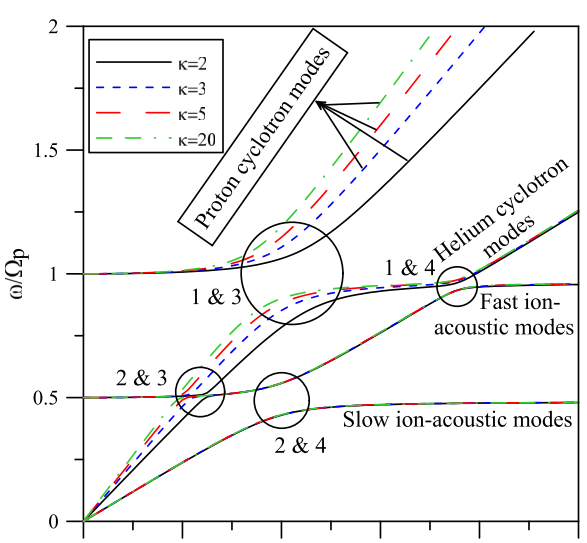

FIG. 5. Dispersion relation curves for varying value of superthermality index, κ, for propagation angle $\alpha = 15°$. The other parameters are the same as in Figure 3.

whereas there is an increase in the frequency and phase speed of the slow ion acoustic mode with the increase in helium ion concentration. For the helium cyclotron mode, there is insignificant effect on the frequency for $k\rho_p \leq 0.3$, whereas frequency increases beyond $k\rho_p \geq 0.3$. The coupling of various modes remains similar to the one described in Figure 3(d).

In Figure 5, the effect of superthermality index, κ, on the various modes is studied. The fixed parameters in this case are $\frac{n_i}{n_e} = 0.05$, $\alpha = 15°$, $\gamma = 3$, $\frac{T_e}{T_p} = 5$, and $\frac{T_i}{T_p} = 2$. The frequency of the proton cyclotron mode is not affected initially (for $k\rho_p \leq 0.2$) with an increase in the superthermality (decrease in κ values); however, for $k\rho_p \geq 0.2$, it decreases for fixed values of $k\rho_p$. Similarly, for the helium cyclotron mode, there is no effect of variation of κ on the frequency of the mode for the wavenumber ranges $k\rho_p \leq 0.2$ and $k\rho_p \geq 0.75$. On the other hand, the frequency of the helium cyclotron mode increases with increase in κ values for the wavenumber ranges $0.2 \leq k\rho_p \leq 0.75$. Further, the frequency of the fast-ion acoustic mode increases with increase in κ values for $k\rho_p \leq 0.25$, and it remains unchanged beyond $k\rho_p \geq 0.25$. The variation of κ does not show any effect on the frequency of the slow-ion acoustic mode. The highest frequency for both the proton and helium cyclotron modes and fast ion-acoustic modes occurs at larger κ values, i.e., for Maxwellian distribution of electrons. These results are consistent with Sultana *et al.*[44] though they have studied ion-acoustic and ion cyclotron waves in two-component, electron-ion magnetized plasma with electrons having κ distribution.

In Figure 6, the general dispersion relation (6) is analyzed for the effect of variation of temperature of ions. The fixed parameters are $n_i/n_e = 0.05$, $\alpha = 15°$, $\gamma = 3$, $\kappa = 2$, and $T_e/T_p = 5$. The ratio of the ion to proton temperature, T_i/T_p, is varied from 2–5 as shown by the legends in the figure. The frequency of the proton cyclotron mode is not affected significantly by the variation of helium ion temperature. There

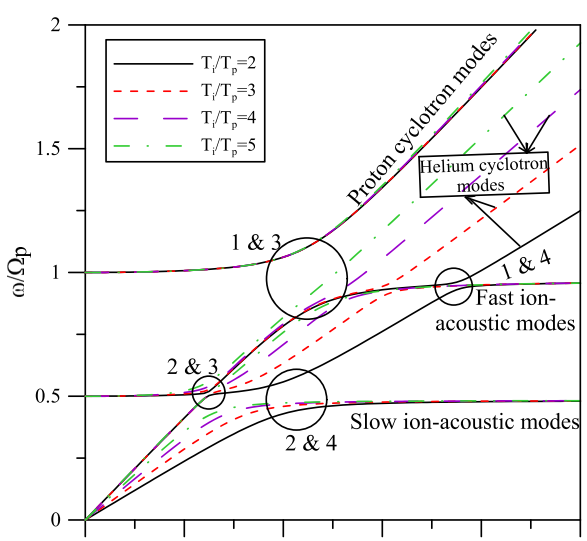

FIG. 6. Effect of $\frac{T_i}{T_p}$ on the dispersion curves for propagation angle $\alpha = 15°$. The other parameters are the same as in Figure 3.

is appreciable increase in the frequency of the helium cyclotron mode with increase in helium ion temperature for $k\rho_p \geq 0.45$, whereas it is slightly affected for $k\rho_p \leq 0.45$. For the fast-ion acoustic mode, the frequency increases with increase in helium ion temperature for $0.25 \leq k\rho_p \leq 0.75$, otherwise it remains unchanged. Similarly, for there is increase in frequency of the slow-ion acoustic mode for $k\rho_p \leq 0.5$, whereas it is not affected for other values of wavenumbers.

IV. DISUSSION AND CONCLUSIONS

Electrostatic ion cyclotron and ion acoustic waves which are observed in solar wind and various regions of the Earth's magnetosphere have been studied in three-component plasma. The plasma model consists of electrons with kappa distributions, protons, and alpha particles. For parallel propagation of the waves, slow and fast ion-acoustic modes and proton and helium-cyclotron modes are decoupled. The proton and helium cyclotron modes are non-propagating modes, whereas the other two modes, i.e., slow and fast ion-acoustic modes, are propagating modes. It is interesting to note that for oblique propagation of the electrostatic waves, the coupling between acoustic and cyclotron modes occurs. For small angle of propagation, there is stronger coupling between proton cyclotron and fast ion acoustic modes, proton cyclotron and slow ion acoustic modes, as well as between helium cyclotron and fast ion acoustic modes and helium cyclotron and slow ion acoustic modes. However, coupling between proton cyclotron and slow ion acoustic modes and helium cyclotron and fast ion acoustic modes is much stronger than between proton cyclotron and fast ion acoustic modes and helium cyclotron and slow ion acoustic modes. Further, for more oblique cases, the coupling between the various modes weakens as the separation between them increases, and for the case of perpendicular propagation of the waves, acoustic (both fast and slow) modes disappear and only proton and helium cyclotron modes remain.

The effect of helium ion concentration is not significant on the frequency of the other modes except for helium cyclotron mode, where its frequency increases beyond $k\rho_p \geq 0.3$ with the increase in helium ion concentration. The frequencies of all modes decrease for certain wave number regimes with an increase in the superthermality (decrease in κ values), except for slow ion acoustic mode for which there is insignificant effect of superthermality. The effect of helium ion temperature is significant on the frequency of helium cyclotron mode, and it increases with increase in temperature. It must be pointed out here that the coupling between the various branches occurs for $k\rho_p < 1$.

We have focussed our attention on the coupling of EIC and ion-acoustic waves which is important in the case of multi-component space and laboratory plasmas. Earlier theoretical studies did not consider the coupling of these modes in either two component or multi-component plasmas. Though we have taken solar wind parameters in this study, however, our results can be generalised and applied to recent observations of coupling of electrostatic ion cyclotron and ion acoustic wave by THEMIS[15] near the magnetopause. The EIC waves are important from the point of view that they can resonantly heat and efficiently transfer energy to the ions in perpendicular direction.

ACKNOWLEDGMENTS

G.S.L. thanks the National Academy of Sciences, India, for the support under the NASI-Senior Scientist Platinum Jubilee Fellowship scheme.

[1]N. D'Angelo and R. W. Motley, Phys. Fluids **5**, 633–634 (1962).
[2]R. W. Motley and N. D'Angelo, Phys. Fluids **6**, 296–299 (1963).
[3]S. R. Mosier and D. A. Gurnett, Nature **223**, 605–606 (1969).
[4]A. Barkan, N. D'Angelo, and R. L. Merlino, Planet. Space Sci. **43**, 905–908 (1995).
[5]A. Lang and H. Boehmer, J. Geophys. Res. **88**, 5564–5572, doi:10.1029/JA088iA07p05564 (1983).
[6]B. Song, D. Suszcynsky, N. D'Angelo, and R. L. Merlino, Phys. Fluids B **1**, 2316–2318 (1989).
[7]S. H. Kim, J. R. Heinrich, and R. L. Merlino, Planet. Space Sci. **56**, 1552–1559 (2008).
[8]P. M. Kintner, M. C. Kelley, and F. S. Mozer, Geophys. Res. Lett. **5**, 139–142, doi:10.1029/GL005i002p00139 (1978).
[9]P. M. Kintner, M. C. Kelley, R. D. Sharp, A. G. Ghielmetti, M. Temerin, C. Cattell, P. F. Mizera, and J. F. Fennell, J. Geophys. Res. **84**, 7201–7212, doi:10.1029/JA084iA12p07201 (1979).
[10]M. Temerin, M. Woldorff, and F. S. Mozer, Phys. Rev. Lett. **43**, 1941 (1979).
[11]C. A. Cattell, F. S. Mozer, I. Roth, R. C. E. R. R. Anderson, W. Lennartsson, and E. Ungstrup, J. Geophys. Res. **96**, 11421–11439, doi:10.1029/91JA00378 (1991).
[12]M. André, H. Koskinen, G. Gustafsson, and R. Lundin, Geophys. Res. Lett. **14**, 463–466, doi:10.1029/GL014i004p00463 (1987).
[13]F. S. Mozer, R. Ergun, M. Temerin, C. Cattell, J. Dombeck, and J. Wygant, Phys. Rev. Lett. **79**, 1281 (1997).
[14]C. Cattell, R. Bergmann, K. Sigsbee, C. Carlson, C. Chaston, R. Ergun, J. McFadden, F. S. Mozer, M. Temerin, R. Strangeway, R. Elphic, L. Kistler, E. Moebius, L. Tang, D. Klumpar, and R. Pfaff, Geophys. Res. Lett. **25**, 2053–2056, doi:10.1029/98GL00834 (1998).
[15]X. Tang, C. Cattell, R. Lysak, L. B. Wilson III, L. Dai, and S. Thaller, J. Geophys. Res. **120**, 3380–3392, doi:10.1002/2015JA020984 (2015).
[16]E. A. Bering, J. Geophys. Res. **89**, 1635–1649, doi:10.1029/JA089iA03p01635 (1984).

[17]E. Ungstrup, D. M. Klumpar, and W. J. Heikkila, J. Geophys. Res. **84**, 4289–4296, doi:10.1029/JA084iA08p04289 (1979).
[18]J. M. Kindel and C. F. Kennel, J. Geophys. Res. **76**, 3055–3078, doi:10.1029/JA076i013p03055 (1971).
[19]J. P. Hauck, H. Böhmer, N. Rynn, and G. Benford, J. Plasma Phys. **19**, 253 (1978).
[20]C. Cattell, J. Geophys. Res. **86**, 3641–3645, doi:10.1029/JA086iA05p03641 (1981).
[21]R. Bergmann, J. Geophys. Res. **89**, 953–968, doi:10.1029/JA089iA02p00953 (1984).
[22]R. L. Kaufmann, G. R. Ludlow, H. L. Collin, W. K. Peterson, and J. L. Burch, J. Geophys. Res. **91**, 10080–10096, doi:10.1029/JA091iA09p10080 (1986).
[23]G. S. Lakhina, J. Geophys. Res. **92**, 12161–12170, doi:10.1029/JA092iA11p12161 (1987).
[24]R. Bergmann, I. Roth, and M. K. Hudson, J. Geophys. Res. **93**, 4005–4020, doi:10.1029/JA093iA05p04005 (1988).
[25]P. B. Dusenbery, R. F. Martin, Jr., and R. M. Winglee, J. Geophys. Res. **93**, 5655–5664, doi:10.1029/JA093iA06p05655 (1988).
[26]G. Ganguli, Y. C. Lee, and P. J. Palmadesso, Phys. Fluids **31**, 823 (1988).
[27]G. Ganguli, S. Slinker, V. Gavrishchaka, and W. Scales, Phys. Plasmas **9**, 2321–2329 (2002).
[28]B. T. Tsurutani and R. M. Thorne, Geophys. Res. Lett. **9**, 1247–1250, doi:10.1029/GL009i011p01247 (1982).
[29]V. W. Chow and M. Rosenberg, Phys. Plasmas **3**, 1202–1211 (1996).
[30]V. W. Chow and M. Rosenberg, Planet. Space Sci. **43**, 613–618 (1995).
[31]J. Sharma and S. C. Sharma, Phys. Plasmas **17**, 123701 (2010).
[32]J. Sharma, S. C. Sharma, and D. Kaur, Prog. Electromagn. Res. Lett. **54**, 123–128 (2015).
[33]J. Sharma, S. C. Sharma, V. K. Jain, and A. Gahlot, J. Plasma Phys. **79**, 577–585 (2013).
[34]M. Kono, J. Vranjes, and N. Batool, Phys. Rev. Lett. **112**, 105001 (2014).
[35]R. L. Merlino, Phys. Plasmas **9**, 1824–1825 (2002).
[36]W. E. Drummond and M. N. Rosenbluth, Phys. Fluids **5**, 1507–1513 (1962).
[37]V. V. Gavrishchaka, S. B. Ganguli, and G. I. Ganguli, J. Geophys. Res. **104**, 12683–12693, doi:10.1029/1999JA900094 (1999).
[38]V. V. Gavrishchaka, G. I. Ganguli, W. A. Scales, S. P. Slinker, C. C. Chaston, J. P. McFadden, R. E. Ergun, and C. Carlson, Phys. Rev. Lett. **85**, 4285–4288 (2000).
[39]D. A. Gurnett and L. A. Frank, J. Geophys. Res. **83**, 58–74, doi:10.1029/JA083iA01p00058 (1978).
[40]D. A. Gurnett, E. Marsch, W. Pilipp, R. Schwenn, and H. Rosenbauer, J. Geophys. Res. **84**, 2029–2038, doi:10.1029/JA084iA05p02029 (1979).
[41]N. Lin, P. J. Kellogg, R. J. MacDowall, and S. P. Gary, Space Sci. Rev. **97**, 193–196 (2001).
[42]M. Backrud-Ivgren, G. Stenberg, M. André, M. Morooka, Y. Hobara, S. Joko, K. Rönnmark, N. Cornilleau-Wehrlin, A. Fazakerley, and H. Rème, Ann. Geophys. **23**, 3739–3752 (2005).
[43]M. A. Hellberg and R. L. Mace, Phys. Plasmas **9**, 1495–1504 (2002).
[44]S. Sultana, I. Kourakis, N. S. Saini, and M. A. Hellberg, Phys. Plasmas **17**, 032310 (2010).
[45]M. N. Kadijani, H. Abbasi, and H. H. Pajouh, Plasma Phys. Controlled Fusion **53**, 025004 (2010).
[46]T. Ohnuma, S. Miyake, T. Watanabe, T. Watari, and T. Sato, Phys. Rev. Lett. **30**, 535 (1973).
[47]R. Bruno and V. Carbone, Living Rev. Sol. Phys. **2**, 1–186 (2005).
[48]E. Marsch, Living Rev. Sol. Phys. **3**, 1–100 (2006).
[49]E. Marsch, K. H. Mühlhäuser, H. Rosenbauer, R. Schwenn, and F. M. Neubauer, J. Geophys. Res. **87**, 35–51, doi:10.1029/JA087iA01p00035 (1982).
[50]M. D. Montgomery, S. J. Bame, and A. J. Hundhausen, J. Geophys. Res. **73**, 4999–5003, doi:10.1029/JA073i015p04999 (1968).
[51]M. Maksimovic, I. Zouganelis, J. Chaufray, K. Issautier, E. Scime, J. E. Littleton, E. Marsch, D. McComas, C. Salem, R. Lin, and H. Elliott, J. Geophys. Res. **110**, A09104, doi:10.1029/2005JA011119 (2005).
[52]W. G. Pilipp, H. Miggenrieder, K.-H. Mühlhäuser, H. Rosenbauer, R. Schwenn, and F. M. Neubauer, J. Geophys. Res. **92**, 1103–1118, doi:10.1029/JA092iA02p01103 (1987).
[53]M. R. Collier, D. C. Hamilton, G. Gloeckler, P. Bochsler, and R. B. Sheldon, Geophys. Res. Lett. **23**, 1191–1194, doi:10.1029/96GL00621 (1996).
[54]K. Chotoo, N. A. Schwadron, G. M. Mason, T. H. Zurbuchen, G. Gloeckler, A. Posner, L. A. Fisk, A. B. Galvin, D. C. Hamilton, and M. R. Collier, J. Geophys. Res. **105**, 23107–23122, doi:10.1029/1998JA000015 (2000).
[55]V. M. Vasyliunas, J. Geophys. Res. **73**, 2839–2884, doi:10.1029/JA073i009p02839 (1968).
[56]M. Maksimovic, V. Pierrard, and J. F. Lemaire, Astron. Astrophys. **324**, 725–734 (1997).
[57]K. Ogasawara, V. Angelopoulos, M. A. Dayeh, S. A. Fuselier, G. Livadiotis, D. J. McComas, and J. P. McFadden, J. Geophys. Res. **118**, 3126–3137, doi:10.1002/jgra.50353 (2013).
[58]N. F. Pisarenko, E. Y. Budnik, Y. I. Ermolaev, I. P. Kirpichev, V. N. Lutsenko, E. I. Morozova, and E. E. Antonova, J. Atmos. Sol.-Terr. Phys. **64**, 573–583 (2002).
[59]C. A. Kletzing, J. D. Scudder, E. E. Dors, and C. Curto, J. Geophys. Res. **108**, 1360, doi:10.1029/2002JA009678 (2003).
[60]P. Schippers, M. Blanc, N. André, I. Dandouras, G. Lewis, L. Gilbert, A. Persoon, N. Krupp, D. Gurnett, A. Coates, and S. Krimigis, J. Geophys. Res. **113**, A07208, doi:10.1029/2008JA013098 (2008).
[61]D. C. Nicholls, M. A. Dopita, and R. S. Sutherland, Astrophys. J. **752**, 148 (2012).
[62]B. Basu and N. J. Grossbard, Phys. Plasmas **18**, 092106 (2011).
[63]D. Summers and R. M. Thorne, Phys. Fluids B **3**, 1835–1847 (1991).
[64]A. Mangeney, C. Salem, C. Lacombe, J.-L. Bougeret, C. Perche, R. Manning, P. J. Kellogg, K. Goetz, S. J. Monson, and J.-M. Bosqued, Ann. Geophys. **17**, 307–320 (1999).
[65]J. E. Borovsky and S. P. Gary, J. Geophys. Res. **119**, 5210–5219, doi:10.1002/2014JA019758 (2014).
[66]M. Maksimovic, V. Pierrard, and P. Riley, Geophys. Res. Lett. **24**, 1151–1154, doi:10.1029/97GL00992 (1997).
[67]G. Livadiotis, J. Geophys. Res. **120**, 1607–1619, doi:10.1002/2014JA020825 (2015).